

# Hydrodynamic Analysis with Heat Transfer in Solid Gas Fluidized Bed Reactor for Solar Thermal Applications

Sam Rasoulzadeh, Atefeh Mousavi

**Abstract**—Fluidized bed reactors are known as highly exothermic and endothermic according to uniformity in temperature as a safe and effective mean for catalytic reactors. In these reactors, a wide range of catalyst particles can be used and by using a continuous operation proceed to produce in succession. Providing optimal conditions for the operation of these types of reactors will prevent the exorbitant costs necessary to carry out laboratory work. In this regard, a hydrodynamic analysis was carried out with heat transfer in the solid-gas fluidized bed reactor for solar thermal applications. The results showed that in the fluid flow the input of the reactor has a lower temperature than the outlet, and when the fluid is passing from the reactor, the heat transfer happens between cylinder and solar panel and fluid. It increases the fluid temperature in the outlet pump and also the kinetic energy of the fluid has been raised in the outlet areas.

**Keywords**—Heat transfer, solar reactor, fluidized bed reactor, CFD.

## I. INTRODUCTION

THE fixed bed reactors have a significant share in the oil, gas, petrochemical and chemical industries, and now most of the gas phase commercial processes are carried out in these reactors. Compared to other types of reactors, fixed bed reactors have been very much considered due to their simple technology and low operating costs [1].

Almost all energy production methods including fluid flow and heat transfer are considered as the main processes. The basis of the fluidized reactors is heat transfer and chemical interactions. Considering the direct effect of heat transfer on the production, it seems that examining the performance of the reactor under different temperature conditions can lead to a better understanding of the heat transfer inside the bed, which will increase the production efficiency. It can be concluded that good quality understanding and accurate quantitative description of heat transfer in fixed bed reactors is necessary for modeling this equipment. For optimal design of reactors, temperature should be predicted in different locations, because the temperature distribution is effective on the efficiency (conversion percent) of the reactor [2].

Researches on the heat transfer of solid gas systems have shown that the hydrodynamics of a bubble bed reactor are

calculated by using CFD. Flow structure and flow pattern changes by changing the size of gas bubbles in a bubble column reactor utilized Lagrangian Trajectory Analysis to investigate the hydrodynamic flow [3].

The most fundamental issue in hydrodynamic modeling of a solid-gas fluidized bed is the movement of two phases in the unknown common interface, and the variables in them, as well as the interaction of two phases on each other. Computational fluids dynamics known as accurate and reliable instruments for better understanding the complex phenomena that occur between the gas phase and particles are. Also, two common approaches for modeling multiphase flows are The Euler–Eulerian approach and Euler-Lagrangian approach. The Euler-Eulerian view is considering as the most probable and commonly used option for modeling fluidized bed issues [4]. The applications of renewable energy in industrial and scientific assemblies are of particular importance and, given that solar energy is clean, it is known as a low-cost energy source, and so far there are various tools in this regard [5]. The suppliers of solar thermal energy are classified by the United States Energy Information Administration in three categories: Low, Medium, and High. At low temperatures, generally flat panels are used in residential areas. In the middle temperature section, flat panels are used, but in high numbers, they are used for heating water or air in business districts. At high temperatures, focused sunlight is used by mirrors and lenses to generate intended electricity [6]. Solid-gas fluidized beds are widely used in the chemical industry, including heat transfer reactors and solar energy, which is in a solid-gas fluidized bed reactor by hydrodynamic [7].

Nowadays, the applications of solar reactors from dense gas-solid fluidized beds, mixing and separation processes play an important role in speed and efficiency of reaction [8]. Significant efforts have been made for developing advanced techniques of measuring dense solid-gas flow dynamics in fluidized beds such as Particle Image Velocity (PIV), Digital Image Analysis (DIA), positron particles tracking, magnetic resonance imaging, electrical capacitor tomography, and so on. However, it is very challenging to obtain accurate flow characteristics at reasonable cost [9]. With the rapid advances in computers and numerical algorithms, CFD has become a powerful tool for obtaining dense solid-gas flow particularity. Euler-Euler and Euler-Lagrange models are the most widely used models. In discrete particles model, particle collisions are modeled by the soft sphere or the hard sphere method. In the early stages, the simulation particles number was only a few

Sam Rasoulzadeh is MSc in Mechanical Engineering, Mechanical Engineering Department, Tehran University, Tehran, Iran (corresponding author, e-mail: sam.rasulzade@gmail.com).

Atefeh Mousavi is MSc in Mechanical Engineering, Science and Research Branch, Islamic Azad University, Tehran, Iran.

thousand, but now with advanced computers and advanced techniques, 100,000 particles can be simulated with a single core processor. With parallel computing, fluidized bed systems with several million particles have been simulated for a variety of issues [10].

Fluidized bed reactors are used as receiver and storage systems of concentrated solar factories which are one of the most promising developing technologies [11]. Solar particle receptors (SPRs) have been developed to deploy centralized solar power stations (CSPs) at higher operating temperatures and increasing the efficiency of power cycles. In the CSP system based on SPR, solid particles are used as a heat transfer media (HTM) instead of salt or liquid vapor [12]. Different numerical and experimental studies were performed to improve the thermal performance of fluidized beds of centralized solar power stations and thermal energy storage programs [13]. In this study, we investigate the heat transfer in the reactor by hydrodynamics in solid gas bed that plays a role in the mixing and separation process and plays a very important role in solar thermal applications.

## II. MATERIALS AND METHODS

### A. Research Method

First, based on the previous researches, a suitable model was chosen for simulation. Then, modeling and simulation of multiphase flow in the reactor was studied through FLUENT software.

### B. Governing Equations

In order to give a general definition for the Law of Mass Conservation, we can say that according to the general Law of Continuity based on the principle of mass conservation, the increase in mass in the control volume is exactly equal to the amount of entry net mass unto the control volume.

According to the Law of Mass Conservation, continuity generally written like below:

$$\nabla \cdot (\rho_{eff} \vec{v}) = 0 \quad (1)$$

Or in other words:

$$\frac{\partial(\alpha_k \rho_k)}{\partial t} + \nabla \cdot (\alpha_k \rho_k \vec{u}_k) = \sum_{p=1, p \neq k}^n S_{pk} \quad (2)$$

$$\sum_k^n \alpha_k = 1 \quad (3)$$

$\rho$  is density,  $\alpha$  is the volume fraction,  $u$  is the velocity vector and  $S_{pk}$  is the mass transfer rate from  $p$  phase to  $k$  phase.

Finally, the continuity equation for an incompressible stream is converted to:

$$\frac{\partial u}{\partial yx} + \frac{\partial v}{\partial y} + \frac{\partial w}{\partial z} = 0 \quad (4)$$

### C. Momentum Conservation Equation or Newton's Second Law

The equation derived from the application of Newton's second law on flow is called the momentum equation. Newton's second law states that the net force entering the fluid is equal to the fluid element mass multiplied by its acceleration.

According to Newton's second law, we study the momentum equation.

The general form of the momentum equation is as follows

$$\nabla \cdot (\rho_{eff} \vec{v} \vec{v}) = -\nabla_p + \nabla \cdot (\mu_{eff} \nabla \vec{v}) + \rho_{eff} \vec{g} \beta (T - T_i) \quad (5)$$

This equation can be represented in the differential form as

$$\frac{\partial}{\partial t}(\rho \vec{v}) + \nabla \cdot (\rho \vec{v} \vec{v}) = -\nabla_p + \nabla \cdot (\bar{\tau}) + \rho \vec{g} + \vec{F} \quad (6)$$

$p$  is the static pressure,  $\bar{\tau}$  is stress tensor,  $\rho \vec{g}$  and  $\vec{F}$  respectively are the force of gravity and external force applied to the body.  $\bar{\tau}$  stress tensor is also expressed as follows:

$$\bar{\tau} = \mu [(\nabla \vec{v} + \nabla \vec{v}^T)] \quad (7)$$

In (7),  $\mu$  and  $I$  respectively are the molecular viscosity and tensor of the unit. The second term on the right is also the volume dilution effect.

Momentum equations are in fact the Navier-Stokes equations governing the Newtonian slippery fluids:

$$\frac{\partial}{\partial t}(\frac{\partial u_i}{\partial t} + u_i \frac{\partial u_i}{\partial x_i}) = -\frac{\partial p}{\partial x_i} + B_i + \frac{\partial}{\partial x_i} [\mu (\frac{\partial u_i}{\partial x_j} + \frac{\partial u_j}{\partial x_i} - \frac{2}{3} \delta_{ij} \frac{\partial u_k}{\partial x_k})] + \frac{\partial}{\partial x_i} (\xi \frac{\partial u_k}{\partial x_k}) \quad (8)$$

### D. Energy Conservation Equation or First Law of Thermodynamics

The energy conservation principle is nothing other than the first law of thermodynamics. The law states that "the change in the energy inside the element of a fluid equals to the intensity of the work done on the element due to internal and external forces plus the net flow of heat through the element."

The general form of energy conservation equation is as:

$$\nabla \cdot (\rho_{eff} c_{p,eff} \vec{v} T) = \nabla \cdot (k_{eff} \nabla T) \quad (9)$$

One can also write the energy conservation in another form:

$$\frac{\partial}{\partial t}(\rho E) + \nabla \cdot (\vec{v}(\rho E + p)) = \nabla \cdot [k_{eff} \nabla T - \sum_j h_j \vec{J}_j + (\bar{\tau}_{eff} \cdot \vec{v})] + S_h \quad (10)$$

In (12),  $\vec{J}_j$  is the diffusive flux of  $J$  species. Also  $k_{eff}$  is effective conductivity which is obtained from:

$$k_{eff} = k + k_t \quad (11)$$

It is notable that  $k_t$  in (13) is turbulent thermal conductivity. The drag energy entered in momentum equations is obtained from:

$$F_D = \frac{C_D \cdot Re_d}{24} \quad (12)$$

$F_D$  is the drag function and has different definitions for different models of drag coefficient.  $C_D$  is also the drag coefficient which is obtained using experimental relationships and experiments. In (17),  $Re_d$  is the Reynolds number for the drag that is obtained from:

$$Re_d = d_p |\vec{V}_d - \vec{V}_c| / \nu_c \quad (13)$$

Heat conductivity coefficient is also related to the temperature and it is defined as follows:

$$\frac{k_{nf}}{k_f} = 1 + 4.4 Re^{0.4} Pr^{0.66} \left(\frac{T}{T_{fr}}\right)^{10} \left(\frac{k_p}{k_f}\right)^{0.3} \phi^{0.66} \quad (14)$$

In (19),  $Re$  is the number of Reynolds nanoparticles,  $Pr$  is Prandtl number of the basic fluid,  $T$  is the nano fluid temperature,  $k_p$  and  $k_f$  respectively are the thermal conductivity coefficient of the nanoparticles and base fluid, and  $\phi$  is the volume fraction of nanoparticles. The Reynolds and Prandtl numbers are also defined for this conduction coefficient as follows:

Prandtl number

$$Pr = \frac{\mu_f}{\rho_f \alpha_f} \quad (15)$$

Reynolds number

$$Re = \frac{2\rho_f k_B T}{\pi \mu_f^2 d_p} \quad (16)$$

#### E. Method of Creating Geometric Model of Studied Structures

In this research, for geometric design, CATIA software is used for modeling the desired plan. For analysis, the intended model was defined to the ANSYS software, and the system was analyzed in the Fluid Flow (CFX) environment.

#### F. Data Collection

To collect information on theoretical foundations and research literature of subject, library's sources, articles, needed books from Latin and Persian, dissertations and especially Latin articles are used, as well as reputable financial magazines, data centers and also global information networks.

#### G. Methods and Instruments of Analyzing Data

Data analysis was performed using Discrete Element Equation Data and Lagrange Equations via Fluent ANSYS Software.

### III. RESULTS

#### A. Designing Geometric Model of Studied Case Structures

In this research, for geometric design, CATIA software is used for modeling the desired plan. For analysis, the intended model was defined to the ANSYS software, and the system was analyzed in the Fluid Flow (CFX) environment.

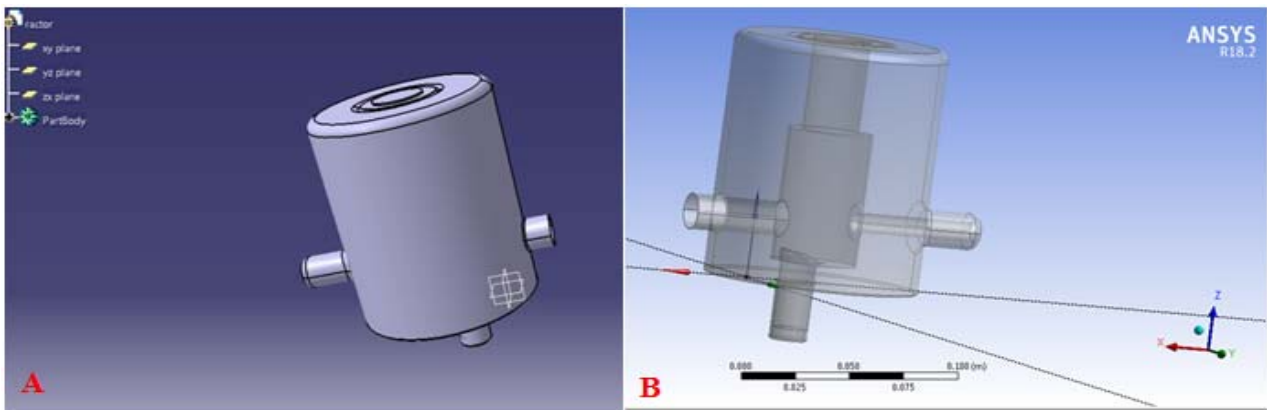


Fig. 1 (A) Initial model in CATIA (B) transferred model in ANSYS

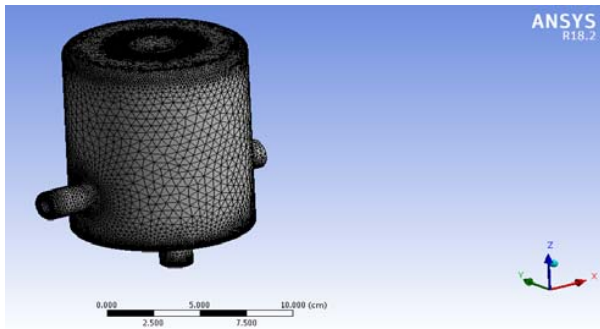


Fig. 2 The model meshing

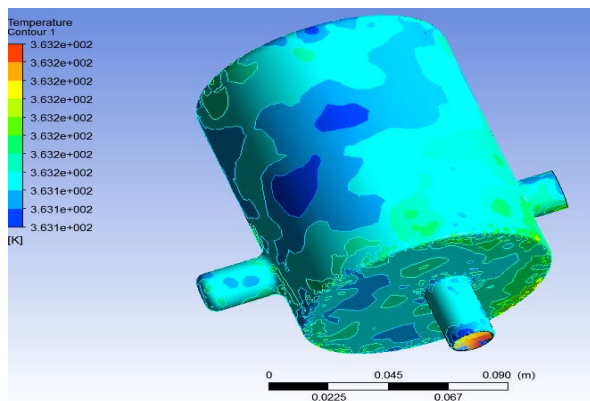


Fig. 3 CFX ANSYS software analysis

### B. The Principles of Mesh

After geometric modeling in the GEOMETRY module, the model enters the MESH module. In this module, meshing was performed once in the software default mode. Then, in areas where irregularities were seen, the structure of the mesh was refined using the REFINEMENT and INFLATION options. One of the important points for meshing is to adjust the size of the elements. The size is chosen largely, the accuracy of the answers will be lowered and on the other hand, if it is small, the required time for solving increases. As a result, depending on the geometry of the model, selecting an appropriate size for the elements is very important. The general rule in setting the element model is that the presence of severe gradients in the used elements reduces the accuracy of the analysis. Therefore, if there are severe gradients in any region, the size of the elements must be fragmented along this gradient. Although there is no definite equation to estimate the number of elements and consequently their size in these particular regions, there are empirical proposals for the production of appropriate mesh with high quality. It should be noted that the size of the elements on the sides of different meshes interface does not differ a lot.

In the next step, we enter the CFX environment and specify the parameters of the input, output and walls of the model. The obtained results after the ANSYS CFX software analysis are in Fig. 3.

TABLE I  
BOUNDARY CONDITIONS OF INPUT FLUID

| Boundary - In      |   |
|--------------------|---|
| Type               | Inlet                                     |
| Location           | In  |
| Setting            |   |
| Flow regime        | Subsonic                                  |
| Heat Transfer      | Static Temperature                        |
| Static Temperature | 2.2000e+01 [C]                            |
| Mass and Momentum  | Normal Speed                              |
| Normal Speed       | 1.0000e+01 [m s <sup>-1</sup> ]           |
| Turbulence         | Medium Intensity and Eddy Viscosity Ratio |
| Fluid              | Fluid 1                                   |
| Volume Fraction    | Value                                     |
| Volume Fraction    | 5.0000e-01                                |
| fluid              | S   |
| Volume Fraction    | Value                                     |
| Volume Fraction    | 5.0000e-01                                |

TABLE II  
BOUNDARY CONDITIONS OF OUTPUT FLUID

| Boundary - out    |                                 |
|-------------------|---------------------------------|
| Type              | OUTLET                          |
| Location          | out                             |
| Setting           |                                 |
| Flow Regime       | Subsonic                        |
| Mass and Momentum | Cartesian Velocity Components   |
| U                 | 1.0000e+00 [m s <sup>-1</sup> ] |
| V                 | 1.5000e+00 [m s <sup>-1</sup> ] |
| W                 | 1.0000e+00 [m s <sup>-1</sup> ] |

TABLE III  
TRANSMISSION OF THERMAL FLUX IN FLUID

| Heat Transfer     | Heat Flux                       |
|-------------------|---------------------------------|
| Heat Flux In      | 1.0000e+01 [W m <sup>-2</sup> ] |
| Thermal Radiation | Opaque                          |
| Diffuse Fraction  | 1.0000e+00                      |
| Emissivity        | 1.0000e+00                      |

### IV. CONCLUSION

In general, the results showed that the flow of fluid in the reactor entrance has less temperature compared with the outlet and when the fluid passes from the reactor, heat transfer happens between cylinder, solar panel and fluid which increases the fluid temperature in the pump outlet. And also, in the outlet zones, the fluid kinetic energy increases.

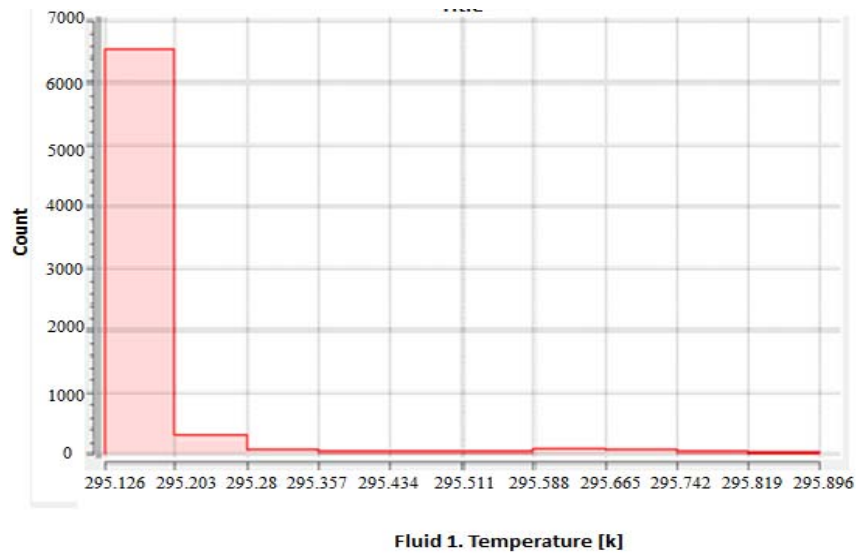


Fig. 4 Histogram of fluid temperature in the reactor

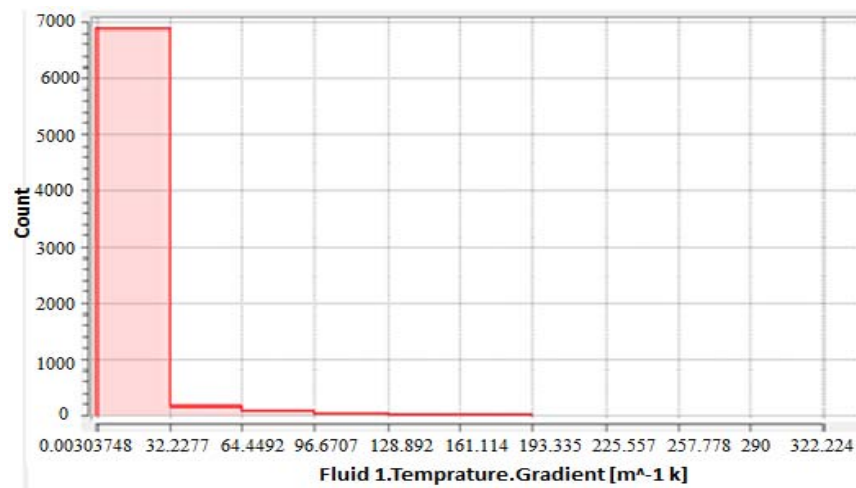


Fig. 5 Histogram of fluid temperature gradient

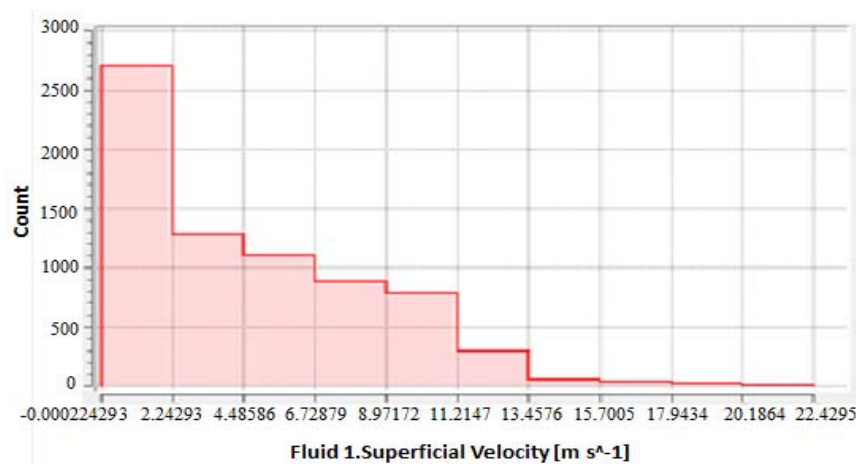


Fig. 6 Histogram of superficial velocity of the fluid

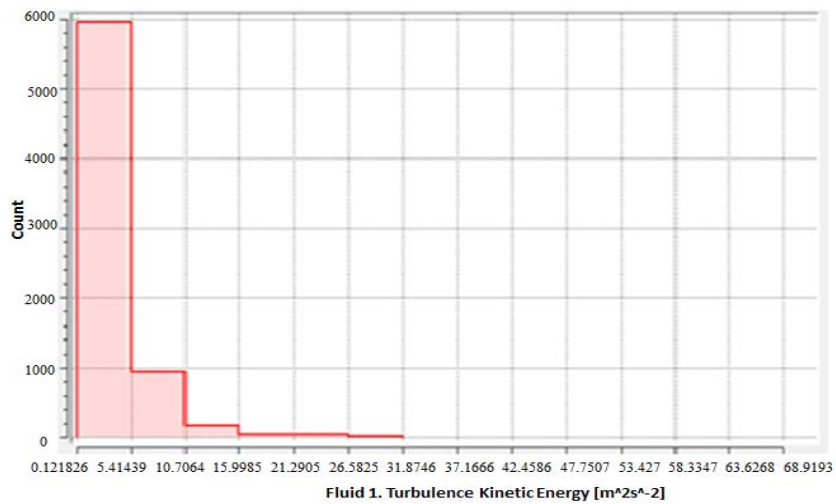


Fig. 7 Histogram of turbulence kinetic energy of fluid

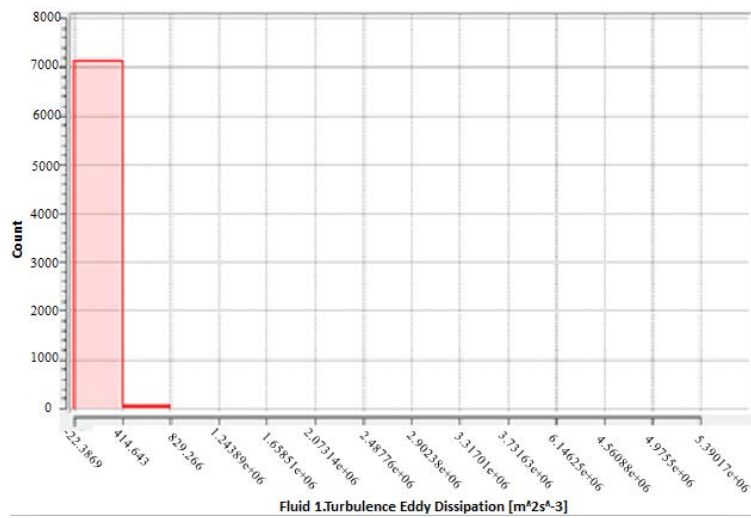


Fig. 8 Histogram of fluid phase change

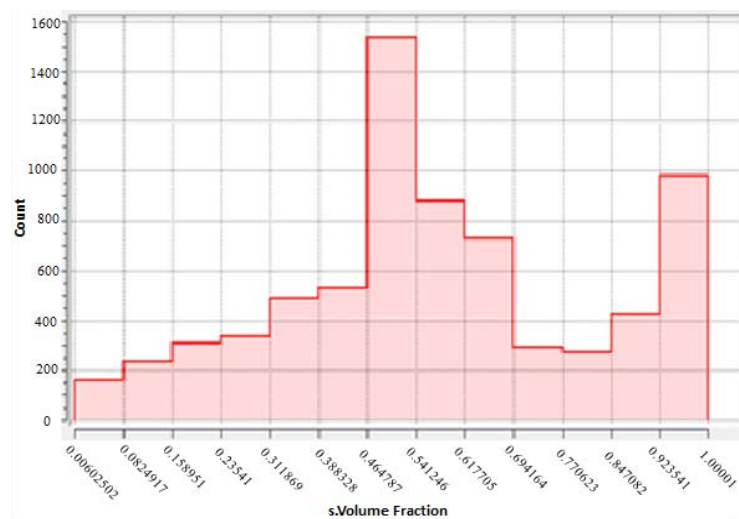


Fig. 9 Histogram of fluid flow kinetic energy

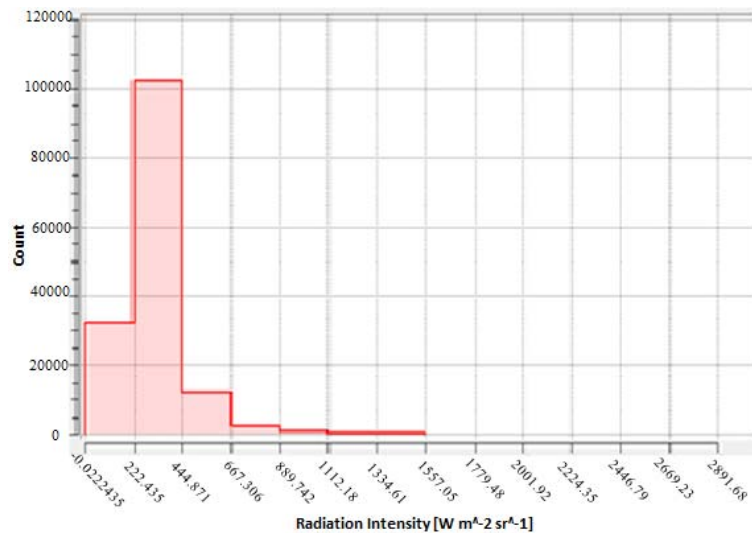


Fig. 10 Histogram of heat flux of fluid and cylinder

## REFERENCES

- [1] F. Bazdidi Tehrani, M. Sedaghat nejad, Ekrami, I. Naeem, Vaasefi, "Single and double phases analysis of mixed nano-fluid transfer in vertical rectangular channel under the heat asymmetric boundary conditions", Elmosannat University, Iran, 2014.
- [2] S. Pahlavani, H. Hashem Abadi, A. Heidari, "CFC simulation of bubble slurry backmix Terephthalic acid producer reactor hydrodynamic", Elmosannat University, Iran, 2014.
- [3] E. Mehrabi Gohari, "Hydrodynamic simulation of a solid-gas fluidized bed by using Boltzman network and uniform profile", 2016.
- [4] A. Khaamesi, R. Abdollah Poursorkhi, M. Pourfalah, "Review of the fluidized bed heat exchangers operation with solar power supply", Mazandaran University of Science and Technology, 2017.
- [5] A. A. Jamali, Sh. Shah Hosseini, "Experimental Investigation and Numerical Simulation of a Three-Phase fluidized bed using Particle Image Tracing", scientific journal of Fluid Mechanics, no. 1, pp.1 -, 2014.
- [6] H. Hosseini, R. Rahimi, M. Zivdar, A. Samimi, "unstable simulation of B kind particles", 2010.
- [7] Y. Behjat, S. Shahhosseini, S. H. Hashemabadi, "CFD modeling of hydrodynamic and heat transfer in fluidized bed reactors", International Communications in Heat and Mass Transfer, 35(3), 357-368, 2008.
- [8] A. Ghaemi, N. Ismail-Zadeh, Sh. Shahhosseini, Y. Behjat, "Simulation of carbon dioxide absorption in a reactor reactor", Faculty of Chemical Engineering, Iran University of Science and Technology, Tehran.
- [9] Q. Wang, Y. Feng, J. Lu, W. Yin, H. Yang, P. J. Witt, M. Zhang, "Numerical study of particle segregation in a coal beneficiation fluidized bed by a TFM-DEM hybrid model: influence of coal particle size and density", *Chemical Engineering Journal*. 260 (2015) 240–257.
- [10] L. Lu, A. Morris, T. Li, S. Benyahia, Extension of a coarse-grained particle method to simulate heat transfer in fluidized beds, *Int. J. Heat Mass Transf.* 111 (2017) 723–735.
- [11] J. R. Van Ommen, R. F. Mudde, Measuring the gas-solids distribution in fluidized beds – a review, *Int. J. Chem. React. Eng.* 6 (2008) 1542–6580.
- [12] Y. Tsuji, T. Kawaguchi, T. Tanaka, Discrete particle simulation of twodimensional fluidized bed, *Powder Technol.* 77 (1993) 79–87.
- [13] H. Zhang, A. Yu, W. Zhong, Y. Tan, A combined TLBM-IBM-DEM scheme for simulating isothermal particulate flow in fluid, *Int. J. Heat Mass Transf.* 91 (2015) 178–189.